STAR Note 331
April 7, 1998

Extracting the Proton $\bar{u}$ Content from pp $\rightarrow$ Direct Photon and Jet Cross Sections

R. G. Badalian
Laboratory of High Energy
Joint Institute for Nuclear Research
141980 Dubna, Moscow Region, Russia

S. Heppelmann
303 Osmond Laboratory
Pennsylvania State University
University Park, Pennsylvania 16802, USA

Abstract

An analysis procedure is proposed to measure the antiquark distributions in the proton over the region $0.01 < x < 0.1$. The procedure involves the measurement of high p_t asymmetric direct photon and jet final states in pp interactions. This measurement can be made at the $RHIC$ collider running in pp mode at an energy of $\sqrt{s} = 500\ GeV/c$. This analysis identifies a region of phase space where the contribution from quark–antiquark annihilation uncharacteristically approaches the magnitude of the contribution from the leading process, quark–gluon Compton scattering. The forward-backward angular asymmetry in the parton center of mass is sensitive to the antiquark content of the proton and the $\bar{u}$ parton density function can be extracted.

I. INTRODUCTION

The distribution functions of quarks and gluons in a proton play a crucial role in the self consistent description of all hard inclusive proton interactions. The cross sections in both lepton–proton and proton–proton high–p_t interactions are derived from the fundamental perturbative QCD parton interaction cross sections, folded with the parton distribution functions and integrated over available phase space. The main sources of experimental input for the parton distribution functions (or structure functions) include deep inelastic lepton–nucleon scattering and hard hadronic inclusive interactions with final states including high mass leptons pairs, high–p_t direct photons, high–p_t jets, W, Z or heavy flavors.

Knowledge of the quark and gluon distributions of the proton has greatly increased in recent years. The first input has come from the high quality data on deep–inelastic structure functions in lepton–nucleon scattering [1,2]. These experiments are generally most sensitive to valence quark distributions. They probe electromagnetically and are only directly sensitive to charged partons rather than gluons. The deep–inelastic scattering experiments have been less conclusive in the determination of the antiquark distributions. Analyses of data to extract the antiquark distributions usually involve various assumptions [3].

Progress in determining the sea quark and gluon distributions in the proton have concentrated on fits to a variety of types of data. The $CTEQ$ Collaboration [4–6] and MRS group [7] have made global fits to available experimental data. But, the determination of the antiquark distributions with hadronic interactions using fit procedures has been difficult because most high–p_t hadronic reactions are either: dominated by contributions from valence partons and gluons; involve too many contributing subprocesses to analyze unambiguously; or have a very small cross section in the high–p_t region. Furthermore, much of the recent high energy collider data involves $\bar{p}p$ interactions where the most probable interactions tend to involve gluons and valence quarks rather than non–valence quarks.

It is unclear how well the antiquark distributions have been determined in the fits by the $CTEQ$ and MRS groups. Even when considering similar data sets, these groups find that their fits differ in the low x region [4]. For example, at $Q^2 = 25\, GeV^2$ the $\bar{u}(x, Q^2)$ distribution from MRS at $x \simeq (0.01 - 0.02)$ is higher by $(10 - 15)\%$ than the same distribution of the $CTEQ$ Collaboration. For the d antiquark $\bar{d}(x, Q^2)$ distribution, this difference increases up to $(15 - 20)\%$ at same region of x and Q^2. It has been difficult to pin down the errors associated with these fits.

To verify and improve the results of these or other fits, measurements which are more directly dependent upon and more sensitive to the antiquark distributions are needed. In this paper, one such experiment and analysis procedure is proposed. A kinematic region is defined for high–p_t direct photon and jet production from pp interactions in which the $u\bar{u}$ annihilation process is uncharacteristically important. The region involves parton pairs with asymmetric momentum fractions and the analysis concentrates on the angular distribution of the parton–parton interaction.

In general, the dominant subprocess for high–p_t direct photon and jet production is the u quark–gluon Compton process. Since the direct photon cross section is proportional to the square of the quark or antiquark charge, the d and s quark contributions are suppressed by a factor of four relative to that of the u quarks. Thus, $u+G \rightarrow u+\gamma$ is the primary subprocess and the next most important process is u and $\bar{u}$ quark annihilation, $u+\bar{u} \rightarrow G+\gamma$. The u quark contribution to direct photon and jet production is enhanced over the d or s quark contributions both because of this factor of four and because of the reduced number of d or s quarks in the proton relative to u quarks.

While the annihilation parton cross section is comparable in magnitude to that of the Compton process, the ratio of the distribution functions $\bar{u}(x)$ to $G(x)$ is typically 1:10 in the region of $x \simeq 0.01 - 0.1$. Generally, the u and $\bar{u}$ annihilation contribution to the direct photon cross section is only about 10%. These two types of parton cross sections do, however, have a different angular distribution.

In the parton model, the direct photon–jet cross section is the sum over subprocess terms, each term is the product of a parton level cross section and the two associated parton density functions. The lowest order partonic cross sections for annihilation and Compton interactions are [8,9]:

$$q+\bar{q} \rightarrow G+\gamma \qquad \Longrightarrow \qquad \frac{d\sigma}{d\hat{t}} \sim \frac{8}{3\,\hat{s}^2}\left(\frac{\hat{t}^2+\hat{u}^2}{\hat{t}\hat{u}}\right) \tag{1}$$

$$q+G \rightarrow q+\gamma \qquad \Longrightarrow \qquad \frac{d\sigma}{d\hat{t}} \sim -\frac{1}{\hat{s}^2}\left(\frac{\hat{s}^2+\hat{u}^2}{\hat{s}\hat{u}}\right), \tag{2}$$

where $\hat{s}$, $\hat{t}$ and $\hat{u}$ are the Mandelstam variables for the parton scattering subprocess.

These two cross sections have very different angular distributions. The Compton cross section is singular for scattering angles corresponding to the u quark scattering backward relative to the incident u quark direction, sending the photon forward. The annihilation process is singular for the photon emerging in the forward or backward direction. The idea of this analysis procedure is to focus on $\gamma+jet$ production in the region of the parton center of mass angular distribution, where the annihilation process is enhanced because of the small $\hat{t}$ singularity.

The variables x_1 and x_2 are defined to be the momentum fractions for the "first" and "second" protons respectively, and ϑ_γ as the angle between the photon and the "first" proton momentum direction in the center of mass of a partonic hard scattering subprocess. Exact definition of "first" and "second" protons will be explained in section III. From observable rapidities η_γ, η_{jet}, the transverse momentum p_t and the pp center of mass energy $\sqrt{s}$, the quantities x_1, x_2 and ϑ_γ are defined as:

$$x_1 = \frac{p_t}{\sqrt{s}}(e^{\eta_\gamma} + e^{\eta_{jet}}) \tag{3}$$

$$x_2 = \frac{p_t}{\sqrt{s}}(e^{-\eta_\gamma} + e^{-\eta_{jet}}) \tag{4}$$

$$\tan\left(\frac{\vartheta_\gamma}{2}\right) = \exp\left(\frac{\eta_{jet}-\eta_\gamma}{2}\right). \tag{5}$$

The forward–backward asymmetry $A(x_1, x_2)$ is then defined as the ratio of the forward to backward cross section:

$$A(x_1, x_2) = \frac{\sigma(\cos(\vartheta_\gamma) > 0.7)}{\sigma(\cos(\vartheta_\gamma) < -0.7)} \tag{6}$$

The choice of $\cos(\vartheta) = \pm 0.7$ as the boundary defining the forward or backward regions, is somewhat arbitrary.

For the two main subprocesses, annihilation and Compton scattering, the forward–backward asymmetry will have a different magnitude. The pair annihilation subprocess $A_{q\bar{q}}(x_1, x_2) = 1$, and the Compton scattering case $A_{qG}(x_1, x_2) \gg 1$. Using this fundamental difference between $A_{q\bar{q}}$ and A_{qG}, the relative strengths of the $\bar{q}(x)$ and $G(x)$ distributions in the proton can be determined.

II. ANALYSIS OF ANGULAR ASYMMETRY

This analysis considers the direct photon and jet production cross section from pp collisions in a small kinematic region defined by $x_1 \pm \Delta x$ and $x_2 \pm \Delta x$ where $x_1 > x_2$. The asymmetric condition $x_1 > x_2$ is important, enabling the observation of the forward–backward asymmetry of the direct photon and jet angular distribution. The proton antiquark density $\bar{u}(x_2)$ will be extracted from the direct photon forward–backward asymmetry in pp collisions as introduced in equation 6.

For illustration, consider the region $x_1 = 0.175 \pm 0.025$ and $x_2 = 0.075 \pm 0.025$. The $\cos(\vartheta_\gamma)$ distributions for the two main subprosses from a $PYTHIA$ simulation of the direct photon and jet production in pp interactions [10] are plotted in figure 1 (a). The pp center of mass energy is $\sqrt{s} = 500\ GeV$ and the events are selected to be in the kinematic region defined by $p_t > 10\ GeV$, $-1 < \eta_\gamma < 2$ and $-1 < \eta_{jet} < 2$ for both the jet and the photon. In the region $\cos(\vartheta_\gamma) > 0.7$ the contribution from the Compton scattering subprocess qG is more then five times greater than the contribution from the pair annihilation subprocess $q\bar{q}$. In contrast, for $\cos(\vartheta_\gamma) < -0.7$ the contribution from the qG–subprocess is only about twice the $q\bar{q}$–subprocess contribution.

The two dimensional plots of the event distributions under the conditions $\cos(\vartheta_\gamma) > 0.7$ and $\cos(\vartheta_\gamma) < -0.7$ are plotted in figure 2 (a) for the same region of $x_1 = 0.175 \pm 0.025$ and $x_2 = 0.075 \pm 0.025$. From the results presented in figure 2, we see that the $\cos(\vartheta_\gamma) > 0.7$ cut selects large photon rapidity and small jet rapidity while the $\cos(\vartheta_\gamma) < -0.7$ cut selects the reverse ordering. Refining the definition of the asymmetry variable to include experimental acceptance, $A(x_1, x_2)$ is to be the accepted cross section (or events number) for $\cos(\vartheta_\gamma) > 0.7$ divided by the accepted cross section $\cos(\vartheta_\gamma) < -0.7$ for a particular (x_1, x_2) bin.

In terms of the parton distribution functions $i(x)$ for parton i and the subprocess differential cross sections $d\sigma_{i,j}/d\cos(\vartheta_\gamma)$ for the process $i + j \to jet + \gamma$, the asymmetry is

$$A(x_1, x_2) = \frac{\sum_{i,j} i(x_1)\, j(x_2)\, \sigma^+_{i,j}}{\sum_{i,j} i(x_1)\, j(x_2)\, \sigma^-_{i,j}} = \frac{\sum_{i,j} N^+_{i,j}(x_1, x_2)}{\sum_{i,j} N^-_{i,j}(x_1, x_2)}\,, \tag{7}$$

where $N^{\pm}_{i,j}(x_1,x_2) = i(x_1)\,j(x_2)\,\sigma^{\pm}_{i,j}$ and $i,\ j = u,\bar{u},d,\bar{d},s,\bar{s},c,\bar{c}$ and G. The cross–sections $\sigma^{\pm}_{i,j}$ are defined as:

$$\sigma^{+}_{i,j} = \int\limits_{\cos(\vartheta_\gamma)>0.7} \frac{d\sigma_{i,j}}{d\cos(\vartheta_\gamma)} d\cos(\vartheta_\gamma) \tag{8}$$

$$\sigma^{-}_{i,j} = \int\limits_{\cos(\vartheta_\gamma)<-0.7} \frac{d\sigma_{i,j}}{d\cos(\vartheta_\gamma)} d\cos(\vartheta_\gamma). \tag{9}$$

In an actual experiment, the divergence at the ± 1 limits of integration will be removed by acceptance and experimental cuts.

It is possible to estimate the asymmetry in the limit of full acceptance, with cross sections dominated by the small t and small u singularities of equations 8 and 9. One can consider only contributions from the u and $\bar{u}$ quarks. A more complete analysis would also include small contributions from $d,\bar{d},s,\bar{s}$ and $c,\bar{c}$ pairs. With these approximations, the asymmetry is given by

$$A(x_1,x_2) \simeq \frac{N^{+}_{u,G} + N^{+}_{G,u} + N^{+}_{u,\bar{u}} + N^{+}_{\bar{u},u} + N^{+}_{\bar{u},G} + N^{+}_{G,\bar{u}}}{N^{-}_{u,G} + N^{-}_{G,u} + N^{-}_{u,\bar{u}} + N^{-}_{\bar{u},u} + N^{-}_{\bar{u},G} + N^{-}_{G,\bar{u}}}\,, \tag{10}$$

where $N^{\pm}_{i,j} = N^{\pm}_{i,j}(x_1,x_2)$, $i,j = u,\bar{u}$ and G. Introducing variables for the ratios of $\bar{u}$ and u quark distribution functions $\bar{u}(x)$ and $u(x)$ to gluons distribution function $G(x)$,

$$r(x) = \frac{\bar{u}(x)}{G(x)}\,, \qquad R(x) = \frac{u(x)}{G(x)}$$

and for the ratio of the integrated Compton cross section to the annihilation cross section, separately for the forward $(+)$ and backward $(-)$ angular regions,

$$B^{\pm} = \frac{\sigma^{\pm}_{u,G}}{\sigma^{\pm}_{u,\bar{u}}}. \tag{11}$$

Noting that $\sigma^{+}_{u,\bar{u}} = \sigma^{-}_{u,\bar{u}}$ and $\sigma^{+}_{u,G} = \sigma^{-}_{G,u} = \sigma^{+}_{\bar{u},G} = \sigma^{-}_{G,\bar{u}}$, the approximate expression for the asymmetry reduces to:

$$A(x_1,x_2;r(x_2)) = \frac{c_2 r(x_2) + c_1 r(x_1) + c_0}{d_2 r(x_2) + d_1 r(x_1) + d_0}\,, \tag{12}$$

where the constants c_i and d_i, $i = 2,1,$ and 0, defined in equation 12, are determined from the well known parton cross sections and u quark and gluon structure functions:

$$c_2 \sim R(x_1) + B^{-}, \qquad d_2 \sim R(x_1) + B^{+}$$

$$c_1 \sim R(x_2) + B^{+}, \qquad d_1 \sim R(x_2) + B^{-}$$

$$c_0 \sim B^+ R(x_1) + B^- R(x_2)\,, \qquad d_0 \sim B^- R(x_1) + B^+ R(x_2)$$

For full acceptance, with cross sections dominated by the singular $\cos(\vartheta_\gamma) = \pm 1$ upper limit of integration, the integrals defined in equations 8 and 9 yield $B^+ = 3/8$ and $B^- = 0$. By restricting the upper limits of integration to $\cos(\vartheta_\gamma) = \pm 0.8$, a more reasonable limit for a measurement at *RHIC*, B^+ increases to about 0.45 and B^- increases to about 0.1. Using these higher values, it is possible to estimate the size and range of observable asymmetries.

Choosing x_1 to be in the region where valence quarks dominate the structure function ($x_1 \simeq 0.2$; $R(x_1) \simeq 0.96$) and choosing x_2 in the region where the gluon distribution dominates ($x_2 \simeq 0.05$; $R(x_2) \simeq 0.25$), the observable range of asymmetry is $2.2 > A(x_1, x_2) > 0.75$. This corresponds to $r(x_2)$ ranging from zero to infinity while holding $r(x_1)$ at a fixed nominal value. For a nominal value of $r(x_2) = 0.088$, $A(x_1, x_2)$ would be about 1.65.

It should be a very general conclusion that the asymmetry will be a ratio of linear functions of $r(x_1)$ and $r(x_2)$ as shown in equation 12. The values of the constants c_i and d_i will be evaluated with the *PYTHIA Monte Carlo* program for various (x_1, x_2) bins, taking into account the experimental acceptance and p_t cutoffs (see section III). It is noted that the dependence of the asymmetry upon the detailed model of the acceptance appears to be modest. The ratio of asymmetries for full acceptance $(0.7 < |\cos(\vartheta_\gamma)| < 1.0)$ to that for the limited acceptance described above $(0.7 < |\cos(\vartheta_\gamma)| < 0.8)$ is only about 3:2, even as the formal cross sections range from infinite to finite. The range of asymmetries for the cuts discussed in the beginning of this section extends from about 0.75 to 2.2 reflecting $\bar{u}(x_2)$ densities ranging from infinity to zero respectively.

It is an important feature of this analysis procedure that the asymmetry is relativitely insensitive to some of the problems which have made the analysis of direct photon data difficult. Accurate modeling of the detector for a rapidly rising cross section near the edge of acceptance in $\cos(\vartheta_\gamma)$ has been one such problem. In this analysis, it is only the ratio of forward to backward efficiencies that must be understood. The price paid for this feature is that the inputs and outputs are not the quark or antiquark structure functions directly but are the ratios of those structure functions to the gluon structure function.

With input from the ratios of quark to gluon structure functions and the ratios of integrated parton Compton cross sections to quark–antiquark annihilation cross sections, the constants c_i and d_i are determined for various (x_1, x_2) regions. These, along with the measured asymmetry $A(x_1, x_2)$, will result in a determination of the antiquark to glue ratio. More specifically, this will determine a well defined combination of $r(x_2)$ and $r(x_1)$, with a rather small coefficient for $r(x_1)$:

$$r(x_2) + \varepsilon r(x_1) = r_\varepsilon\,, \tag{13}$$

where ε and r_ε are determined from the constants c_i, d_i and the value of asymmetry $A(x_1, x_2)$:

$$\varepsilon = \frac{c_1 - d_1 A(x_1, x_2)}{d_2 A(x_1, x_2) - c_2}\,, \qquad r_\varepsilon = \frac{c_0 - d_0 A(x_1, x_2)}{d_2 A(x_1, x_2) - c_2}.$$

By considering different regions (x_1, x_2), each providing a linear equation in $r(x_1)$ and $r(x_2)$, unambiguous analysis should be possible. Unless the ratio $r(x)$ grows rapidly with x in the region $x_2 < x < x_1$, in contradiction of the conventional structure function sets, the effect of the $r(x_1)$ term is small, $\varepsilon \simeq 0.1$ (see section III). It is in this sense, that the asymmetry $A(x_1, x_2)$ is a rather direct measurement of $r(x_2) = \bar{u}(x_2)/G(x_2)$.

III. PYTHIA SIMULATION

In this section we present a discussion of the $p{+}p \to \gamma{+}jet$ process at $\sqrt{s} = 500\,GeV$ based on the *PYTHIA* simulation code [10]. The kinematic cuts are $p_t > 10\,GeV$, $-1 < \eta_\gamma < 2$ and $-1 < \eta_{jet} < 2$, where η_γ and η_{jet} are pseudo-rapidity of the direct photon and jet, respectively. The p_t cut is high enough to provide a fairly clean measurement of a direct (hard) photon with a managable background from π^0 and η meson decay. The η_γ and η_{jet} pseudo-rapidity cuts are consistent with the *STAR* detector acceptances assuming a *Barrel* and an *Endcap Electro–magnetic Calorimeter* (*EMC*).

With one *Endcap EMC*, the *STAR* detector acceptance in pseudo-rapidity has a natural asymmetry – the position of the *Endcap EMC* in the pseudo–rapidity axis $1 < \eta < 2$. Thus, the symmetry between two proton beam directions is broken and the side with the *Endcap* is defined to be at positive displacement from the interaction point and to have acceptance for positive rapidity. The convention will be that x_1 is defined to be a momentum fraction of partons in the beam which moves in the positive direction, consistent with equations 3–5.

The cross section for the direct photon plus jet production in the kinematic region defined by these rapidity cuts are shown for various (x_1, x_2) bins in table I. In table II and table III the cross sections from the two main subprocesses, pair annihilation and the Compton scattering, are shown. The total direct photon and jet production cross section over this region is 9.3 *nb*.

Figure 3 shows the accepted cross section distribution of x_1 and x_2. As shown in figure 3, the pair annihilation contribution to the direct photon and jet production cross section is less than 10% (see, also, tables II and III). Two dimensional distributions of x_1 and x_2 are shown in figure 4. The asymmetry between x_1 and x_2 reflects the asymmetric pseudo–rapidity cuts: $-1 < \eta_{jet} < 2$ and $-1 < \eta_\gamma < 2$, reflecting the *STAR* $Barrel + Endcap$ coverage.

The four small squares in figure 4 are the regions analyzed in this paper. The values of constants c_i, d_i normalized by $d_2 = 1$, ε and values of asymmetry $A(x_1, x_2)$ from these four regions are presented in table IV. Also presented in table IV is the accuracy of the predicted asymmetry $A(x_1, x_2)$ from *PYTHIA Monte Carlo* simulation code. The $\cos(\vartheta_\gamma)$ distributions of the events from these four regions are presented in figure 1.

The minimum value of x_2, consistent with the cuts mentioned above in rapidity, p_t and $\cos(\vartheta_\gamma)$, is $x_2^{min} \simeq 0.02$. The choice of a $\cos(\vartheta_\gamma)$ limit value of 0.7 is a trade–off between the need for a large asymmetry $A(x_1, x_2)$ and for a sufficiently large cross section. Reduction of the p_t limit would provide coverage in regions of $x_2 < 0.02$.

Lower x_2 can also be reached by decreasing the $\cos(\vartheta_\gamma)$ limit. If asymmetry was defined by $|\cos(\vartheta_\gamma)| > 0.5$, there is sensitivity down to $x_2^{min} \simeq 0.01$ with the same p_t cut. Such a choice involves larger accepted cross sections but weaker dependence of asymmetry upon the anti–quark ratio.

The dependence of the forward–backward asymmetry upon $r(x_2)$ is presented in figure 5. The point at $r(x_2) \simeq 0.088$ corresponds to the nominal $CTEQ2L$ structure function sets which were used in $PYTHIA$ (see figure 6). For the four (x_1, x_2) regions considered here, when the nominal $r(x_2) \simeq 0.088$ is assumed, the calculated asymmetries range from about 1.5 to 2.0.

IV. ANALYSIS OF ERRORS

To compare event rates for a variety of experiments at $RHIC$ involving proton–proton colliding beams, $RHIC$ experimentalists have agreed to consider a standard set of integrated luminosities and energies. At center of mass energy $\sqrt{s} = 500\ GeV$, the standard luminosity of $800\,pb^{-1}$ is used to evaluate the expected statistical error. The fractional statistical error, $\delta A/A$, for the four regions considered is presented in table IV. The typical statistical error in measurement of $\delta A/A$ will be about 1%. The corresponding error introduced in the determination of $\delta r(x_2)/r(x_2)$ will be in the (3–7)% range (see figure 7), depending upon the actual value of $r(x_2)$.

Systematic errors will be larger than statistical errors. The systematic errors in the determination of $r(x_2)$ will come from various sources. The important systematic error sources will involve uncertainties in the determination of the constants in equations 12 and 13 and in the interpretation of the various sources of background. The following sources of errors have been considered.

1. **Contribution from partons other that u quarks and gluons G.** The effect on asymmetry from all the other quarks and antiquark processes is small and calculable. Using the standard $CTEQ2L$, the scale for the change in asymmetry $A(x_1, x_2)$ due to the inclusion of other quarks and antiquarks is about 5 %. Even approximate simulation of these contributions would introduce a small uncertainty, $\delta A/A < 1\%$.

2. **Uncertainty in determination of c_i and d_i.** The inputs to this analysis are the ratio of up quark to gluon structure functions $R(x)$. It will be assumed that the ratios can be determined to 10%. As seen in figure 7, this implies an error in the (15–20) % at $x_2 \simeq 0.025$ and (30–40) % at $x_2 \simeq 0.075$ range for $r(x_2)$. As mentioned above, the sensitivity to the detailed acceptance model near the limits of acceptance in rapidity and p_t is not great.

3. **Effects from beyond Leading Order calculations.** The main effect of the higher order corrections will be to increase the cross section by a K–factor. While this is a large increase in cross section, the asymmetry $A(x_1, x_2)$ is insensitive to the normalization. A full higher order calculation would determine a higher order

correction to $A(x_1, x_2)$ and the analysis procedure can be modified to take this into account.

It was seen that in a *Next to Leading Order* (NLO) calculation of the CDF direct photon cross section [11], the change in the $\cos(\vartheta_\gamma)$ dependence is only at the 10% level. This suggests that the sensitivity of $A(x_1, x_2)$ to a full NLO calculation may be rather modest.

4. **Background from jet fragmentation to high–p_t photons.** The standard background to direct photons is from unmatched photons from π^0 decays. Techniques have been developed to correct for this background [12]. It will be assumed here that the cross section of this background source can be directly measured and subtracted. Techniques for this analysis are well developed and will not be discussed here as a source of error in this analysis.

   The background from photons produced directly in the jet fragmentation process is more difficult to estimate and subtract. The CDF analysis of direct photon plus jet production in $p\bar{p}$ interactions shows that the angular dependence is relatively enhanced, in the forward–backward angle regions, over the NLO prediction. The angular distribution is enhanced beyond that predicted in NLO by about $\sim (15-30)\%$ in the region $\cos(\vartheta_\gamma) > 0.5$ [13]. They attribute this discrepancy to an underestimate of the fragmentation function of jets into photons, a calculation done only in leading order. This is about the level of modification expected for a full NLO calculation of jet fragmentation.

   It is reasonable to assume, that the contamination of the direct photon signal from jet fragmentation will be symmetric in $\cos(\vartheta_\gamma)$. This assumption can be checked by a full NLO calculation of jet fragmentation into photons. For example, if the contamination was about 30% and symmetric in $\cos(\vartheta_\gamma)$, $A(x_1, x_2)$ would be reduced from about 2.0 to about 1.63. If the correction was known to be $(30 \pm 10)\%$, the error would be $\delta A/A < 7\%$.

5. **Effects from k_t.** A source of theoretical and experimental discrepancy is the initial state transverse momentum prior to a hard parton collision. An analysis of direct photon data [14] suggests that this k_t distribution is broader than expected, with a width as large as $(2-3)GeV/c$ in this kinematic region of interest. Folded with the rapidly falling p_t dependence, this results in an excess cross section at the lower limit of p_t. In an analysis which anticipates a cross section proportional to the structure function, this is a great complication.

   The crucial point here is that it is not $\bar{u}(x)$ which is measured in this analysis but the ratio $r(x) = \bar{u}(x)/G(x)$. This observable is likely to be a more slowly varying function of x than the structure functions themselves in the small x region. For the analysis described here, a 50% increase in the cross section due to these effects would not be much of a problem. The main effect would be to increase the uncertainty of x_2, somewhat smearing the bin over which the ratio $r(x_2)$ is determined. The resulting error in x_2 is $\delta x_2/x_2 \simeq (10-20)\%$. We have shown that the asymmetry $A(x_1, x_2)$ varies rather slowly with x_2 for the cases considered. It is noted in equation 3 that the ratio of x_1/x_2 is well determined by the rapidity and is not very sensitive to k_t smearing.

It appears, that with reasonable expectations of an eventual complete set of NLO calculations, the largest source of error will come from the uncertainty in $R(x) = u(x)/G(x)$. It does not seem too optimistic to expect a determination of $r(x) = \bar{u}(x)/G(x)$ to an accuracy of $(15 - 30)\%$, at several values of x in the 0.02 to 0.1 region, using this method of analysis. The uncertainty in this measurement of the $\bar{u}$ structure function will be limited by the uncertainty in the u quark and gluon distributions.

It is important to consider the significance of this new source of input into the antiquark structure function fits. In fits to the $\bar{u}(x)$ distribution in this region of Q^2, the main constraints come from high p_t data for processes involving antiquarks and from the measured gluon distribution. The gluon distribution contributes a common component to all the sea quark distributions through evolution. The retio of $\bar{u}(x)/G(x)$ emphasizes the part of $\bar{u}(x)$ which is not derived from the gluon density, the part which distinguishes the $\bar{u}$ from the $\bar{d}$ or the $\bar{s}$ distributions. From current parton parametrizations, the $\bar{u}$ distribution is about twice as large as the $\bar{s}$ distribution in the region considered here. This indicates that for $\bar{u}$ quarks, most of the structure function does not come from gluon evolution and thus can only be constrained with experimental data with quark–antiquark processes.

Experimental input into global fits for the $\bar{u}$ density in this region is currently limited to lower Q^2 Drell–Yan data. From $CTEQ$, MRS or other parton function fits, it is difficult to estimate the uncertainty in the determination of in the $\bar{u}$ structure function. It would not be correct to assume that the errors correspond to the degree of variation among these fits since the input and most of the assumptions are common. A 20% measurement from direct photons is probably significant relative to the current determination and would, in any case, serve as a cross check to the Drell–Yan input and constrain the fits with a measurement involving a distinct set of experimental biases and corrections. Verification of consistency between direct photon and the traditional Drell–Yan processes would provide an experimental test for the calculations of higher order corrections in both processes.

V. SPIN DEPENDENCE

The greatest interest in pp measurements at $RHIC$ involves measurements with polarized beams. With longitudinally polarized beams, the dependence of the cross section on beam polarization can be measured to determine the polarization of the quarks and gluons within the proton. Another asymmetry, A_{LL}, is defined to be the difference between the cross section for spin aligned and anti-aligned protons. This quantity is sensitive to the polarized parton distributions. A region is considered which is centered about (x_1, x_2), with an unpolarized cross section $\sigma(x_1, x_2)$ given by the average of two polarized cross sections $\sigma^{\uparrow\uparrow}(x_1, x_2)$ and $\sigma^{\uparrow\downarrow}(x_1, x_2)$, corresponding to longitudinal spins aligned or anti–aligned respectively. $A_{LL}(x_1, x_2)$ is:

$$\begin{aligned} A_{LL}(x_1, x_2) &= \tfrac{\sigma^{\uparrow\uparrow}(x_1,x_2)-\sigma^{\uparrow\downarrow}(x_1,x_2)}{\sigma^{\uparrow\uparrow}(x_1,x_2)+\sigma^{\uparrow\downarrow}(x_1,x_2)} \\ &= \textstyle\sum_{i,j} P_i^L(x_1) P_j^L(x_2) f_{i,j}(x_1, x_2) a_{i,j}^{LL}(\cos(\vartheta_\gamma)) \end{aligned} \tag{14}$$

where $f_{i,j}(x_1, x_2)$ is the ratio of the unpolarized cross section from partons i and j to the sum of all processes in the region (x_1, x_2), $P_i^L(x)$ is the longitudinal polarization of a parton of type i at momentum fraction x relative to the longitudinal spin of the proton, and $a_{i,j}^{LL}$ is the parton level analyzing power for this subprocess which can depend on the parton center of mass scattering angle. For annihilation and Compton scattering, the analyzing power is [15]:

$$a_{q\bar{q}}^{LL} = a_{\bar{q}q}^{LL} = -1 \tag{15}$$

and

$$a_{qG}^{LL} = a_{\bar{q}G}^{LL} = \frac{\hat{s}^2 - \hat{u}^2}{\hat{s}^2 + \hat{u}^2} = \frac{4 - (1 - \cos(\vartheta_\gamma))^2}{4 + (1 - \cos(\vartheta_\gamma))^2} \tag{16}$$

$$a_{Gq}^{LL} = a_{G\bar{q}}^{LL} = \frac{\hat{s}^2 - \hat{t}^2}{\hat{s}^2 + \hat{t}^2} = \frac{4 - (1 + \cos(\vartheta_\gamma))^2}{4 + (1 + \cos(\vartheta_\gamma))^2} \tag{17}$$

If the magnitude of the anti–up quark structure function is near the nominal value $r(x_2) \simeq 0.1$, then it is interesting to consider A_{LL}^+ and A_{LL}^- defined from considering cases of $\cos(\vartheta_\gamma) > 0.7$ and $\cos(\vartheta_\gamma) < -0.7$ respectively. Considering only the two most important terms in the sum from equation 14,

$$\begin{aligned} A_{LL}(x_1, x_2) \simeq\ & P_u(x_1) P_G(x_2) f_{u,G}(x_1, x_2) a_{u,G}^{LL}(\cos(\vartheta_\gamma)) \\ & + P_u(x_1) P_{\bar{u}}(x_2) f_{u,\bar{u}}(x_1, x_2)(-1) \end{aligned} \tag{18}$$

Many of the factors in equation 18 are to some degree known. In the region of x_1 considered here, $P_u(x_1) \simeq 0.3$ [16,17]. The functions $f_{i,j}(x_1, x_2)$ are the fractional contribution from a process involving i and j in the initial state and can be evaluated in $PYTHIA$.

The result is that in the forward region, the gluon polarization which is also measured in other kinematic regions will be nearly proportional to A^+_{LL}. However, in the backward photon region, A^-_{LL} will be as sensitive to the anti-up quark polarization as to the gluon polarization. Including a degradation of the signal from finite (70%) beam polarization, a 0.5% measurement of A^-_{LL} would be required to determine $P_{\bar{u}}(x_2)$ with an error of about $\delta P_{\bar{u}}(x_2) \simeq \pm 0.1$.

It is interesting to consider the complimentary spin asymmetry with transversely polarized beams, A_{NN}. The formulas differ from that of the longitudinal asymmetry in two ways. First, the observed transverse asymmetry is also proportional to $\sin(\varphi)$, with φ the azimuthal angle of the production plane relative to the transverse polarization axis. Second, there is no contribution to the transverse asymmetry from processes with gluons, therefore the leading source of transverse asymmetry should be the anti–up quark annihilation process, which will have a parton level analyzing power of -1. In the case of transverse polarization, none of the quark polarizations are known so detailed predictions are not very constrained, however, the sensitivity to polarization could be similar to what is described above for longitudinal $\bar{u}$ polarization in this region.

VI. ACKNOWLEDGMENTS

This work has been supported in part by grant *RFFI* # 95–02–05061 from the Russian Academy of Science and the National Science Foundation.

REFERENCES

[1] *H1 Collab.*, S. Aid *et al.*, Nucl. Phys. **D470**, 3 (1996).

[2] *ZEUS Collab.*, M. Derrick *et al.*, Z. Phys. **C69**, 607 (1996); preprint DESY 96 - 076 (1996), Z. Phys., to be published.

[3] D. W. Duke and J. F. Owens, Phys. Rev. **D30**, 49 (1984).

[4] H. L. Lai *et al.*, Phys. Rev. **D51**, 4763 (1995).

[5] J. Botts *et al.*, Phys. Lett. **B304**, 159 (1993).

[6] J. G. Morfin and W. K. Tung, Z. Phys. **C52**, 13 (1991).

[7] A. D. Martin, R. G. Roberts and W. J. Stirling, Phys. Lett. **B387**, 419 (1996); *ibid.* **B356**, 89 (1995); *ibid.* **B354**, 155 (1995); Phys. Rev. **D50**, 6734 (1994).

[8] F. Halzen and D. M. Scott, Phys. Rev. **D18**, 3378 (1978).

[9] J. F. Owens, Rev. Mod. Phys. **59**, 465 (1987).

[10] T. Sjöstrand, Comput. Phys. Commun. **82**, 74 (1994).

[11] *CDF Collab.*, F. Abe *et al.*, Phys. Rev. Lett. **71**, 679 (1993).

[12] *CDF Collab.*, F. Abe *et al.*, Phys. Rev. Lett. **73**, 2662 (1996); *ibid.* **68**, 2734 (1992).

[13] *CDF Collab.*, L. Nodulman, *28th International Conference on High Energy Physics (ICHEP '96)*, Warsaw, Poland, July 1996; FERMILAB - Conf - 96/337 - E (1996).

[14] J. Huston *et al.*, preprint MSU - HEP - 41027, CTEQ - 407 (1995).

[15] C. Bourrely *et al.*, Phys. Rep. **177**, 319 (1989).

[16] *SLAC E - 80*, M. J. Alguard *et al.*, Phys. Rev. Lett. **37**, 1261 (1976); *ibid.* **41**, 70 (1978).
SLAC E - 130, G. Baum *et al.*, Phys. Rev. Lett. **51**, 1135 (1983).

[17] *EMC*, J. Ashman *et al.*, Phys. Lett. **B206**, 364 (1988); Nucl. Phys. **B328**, 1 (1989).

TABLES

Δx_1 / Δx_2	$.00-.05$	$.05-.10$	$.10-.15$	$.15-.20$	$.20-.25$	$.25-.30$	$.30-.35$	$.35-.40$
$.00-.05$	426	1,640	1,457	1,063	663	355	173	85
$.05-.10$	1,263	812	264	112	51	26	13	7.2
$.10-.15$	365	154	45	20	9.0	5.3	2.9	1.8
$.15-.20$	70	42	13	4.8	2.5	1.5	0.64	0.49

TABLE I. Cross sections in picobarns of the direct photon and jet production process.

Δx_1 / Δx_2	$.00-.05$	$.05-.10$	$.10-.15$	$.15-.20$	$.20-.25$	$.25-.30$	$.30-.35$	$.35-.40$
$.00-.05$	26	158	162	128	80	44	22	11
$.05-.10$	124	116	44	20	8.4	4.8	2.8	1.2
$.10-.15$	38	23	7.4	3.3	1.9	1.3	0.73	0.20
$.15-.20$	7.0	6.5	1.9	0.73	0.26	0.23	0.20	0.15

TABLE II. Cross sections in picobarns from the annihilation subprocess.

Δx_1 / Δx_2	$.00-.05$	$.05-.10$	$.10-.15$	$.15-.20$	$.20-.25$	$.25-.30$	$.30-.35$	$.35-.40$
$.00-.05$	400	1,482	1,295	935	582	311	152	74
$.05-.10$	1,138	697	220	91	42	21	10	6.0
$.10-.15$	328	131	37	16	7.1	4.0	2.2	1.6
$.15-.20$	63	35	11	4.1	2.2	1.2	0.64	0.35

TABLE III. Cross sections in picobarns from the Compton scattering subprocess.

x_1 and x_2	σ^+ (pb)	σ^- (pb)	ε	c_2	c_1	c_0	d_1	d_0	$A(x_1, x_2)$	$\delta A/A$ (%) $PYTHIA$	$\delta A/A$ (%) $STAR$ run
$0.175, 0.075$	18.7	13.0	0.13	0.68	0.59	0.27	0.34	0.15	1.44	3.8	1.3
$0.225, 0.075$	9.0	5.6	0.03	0.75	0.49	0.29	0.28	0.13	1.61	5.5	1.9
$0.175, 0.025$	33.9	19.0	0.12	0.70	0.49	0.31	0.20	0.13	1.78	2.9	1.0
$0.225, 0.025$	10.4	5.5	0.06	0.84	0.44	0.33	0.19	0.13	1.87	5.4	1.9

TABLE IV. Cross sections and prediced asymmetry $A(x_1, x_2)$ parameters, $d_2 = 1$.

FIGURES

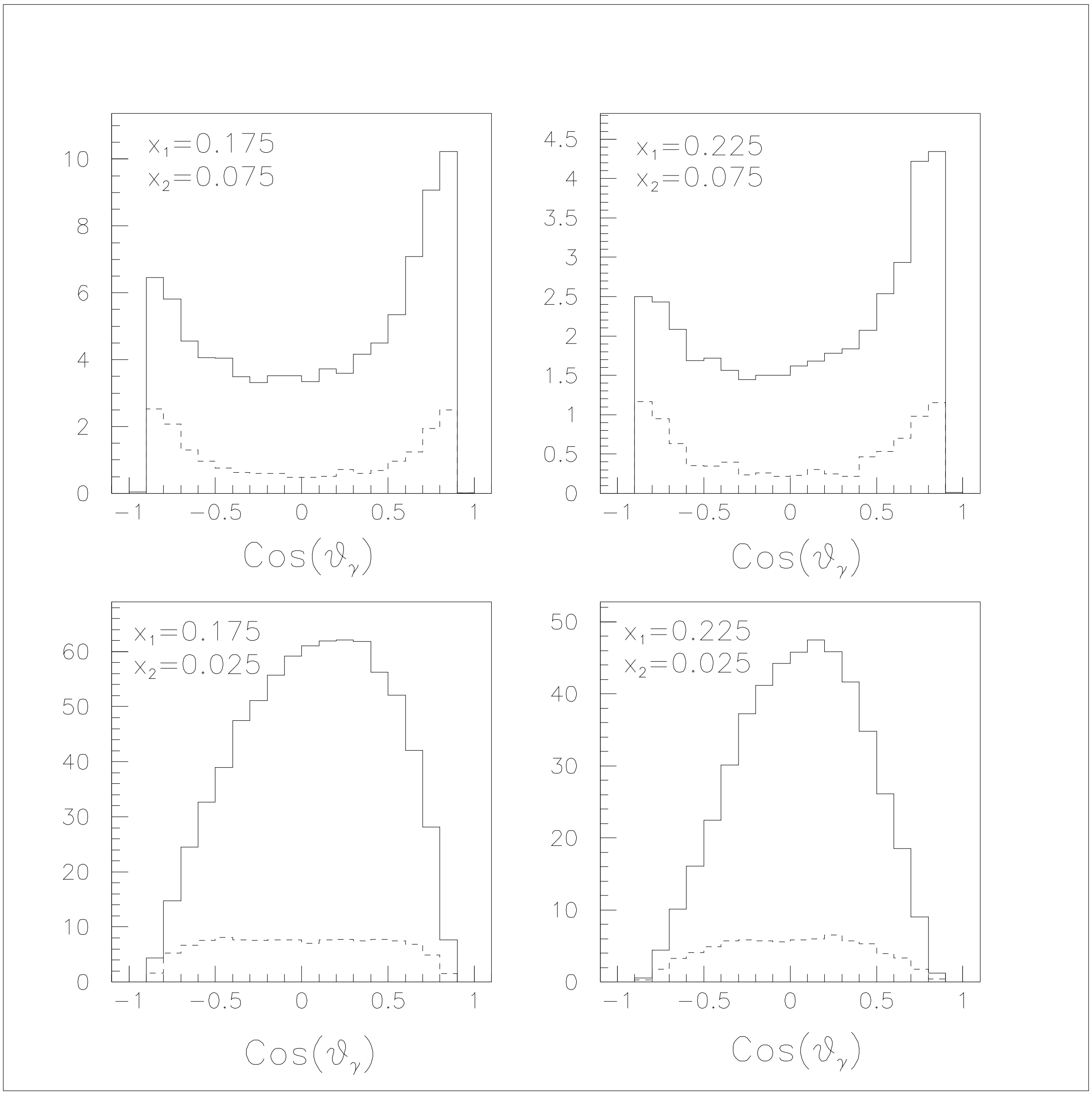

FIG. 1. The $\cos(\vartheta_\gamma)$ distributions at four points of (x_1, x_2) from the reaction $pp \to \gamma + jet$ at pp center of mass energy 500 GeV and $p_t > 10$ GeV in the acceptances of $-1 < \eta_\gamma < 2$ and $-1 < \eta_{jet} < 2$ for photon and jet respectively: a – $x_1 = 0.175, x_2 = 0.075$; b – $x_1 = 0.225, x_2 = 0.075$; c – $x_1 = 0.175, x_2 = 0.025$ and d – $x_1 = 0.225, x_2 = 0.025$. Solid curves – Compton scattering subprocess, dashed curves – pair annihilation subprocess. The numbers in the vertical axis are cross sections in picobarns.

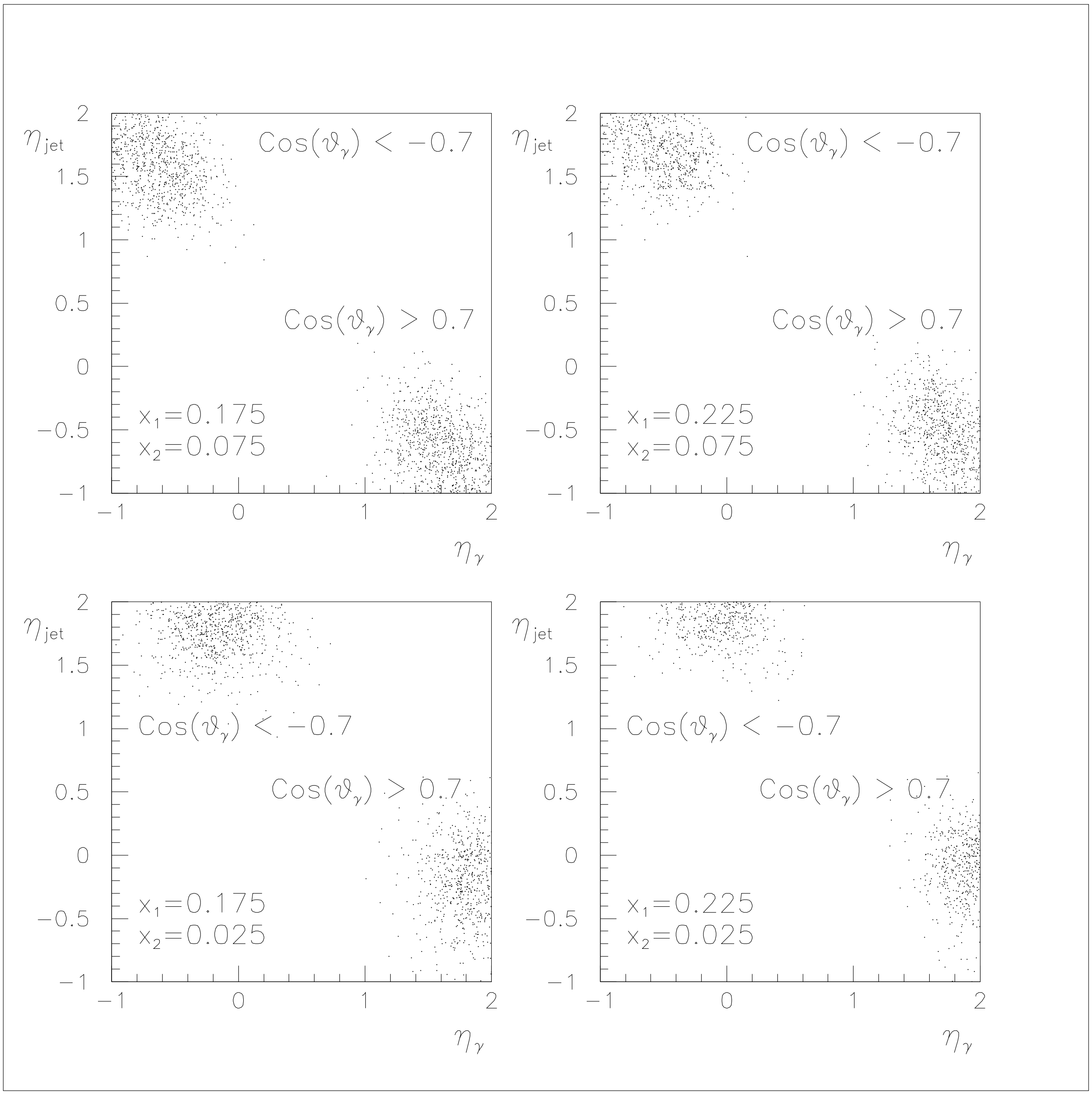

FIG. 2. Events distributions on a $(\eta_\gamma \times \eta_{jet})$ plot from the reaction $pp \to \gamma + jet$ at pp center of mass energy 500 GeV and $p_t > 10$ GeV in the acceptances of $-1 < \eta_\gamma < 2$ and $-1 < \eta_{jet} < 2$ for photon and jet respectively at four points of (x_1, x_2): a − $x_1 = 0.175 \pm 0.025$, $x_2 = 0.075 \pm 0.025$; b − $x_1 = 0.225 \pm 0.025$, $x_2 = 0.075 \pm 0.025$; c − $x_1 = 0.175 \pm 0.025$, $x_2 = 0.025 \pm 0.025$ and d − $x_1 = 0.225 \pm 0.025$, $x_2 = 0.025 \pm 0.025$. In the top part of the figures events are from $\cos(\vartheta_\gamma) < -0.7$ and in the bottom part of the figures from $\cos(\vartheta_\gamma) > 0.7$.

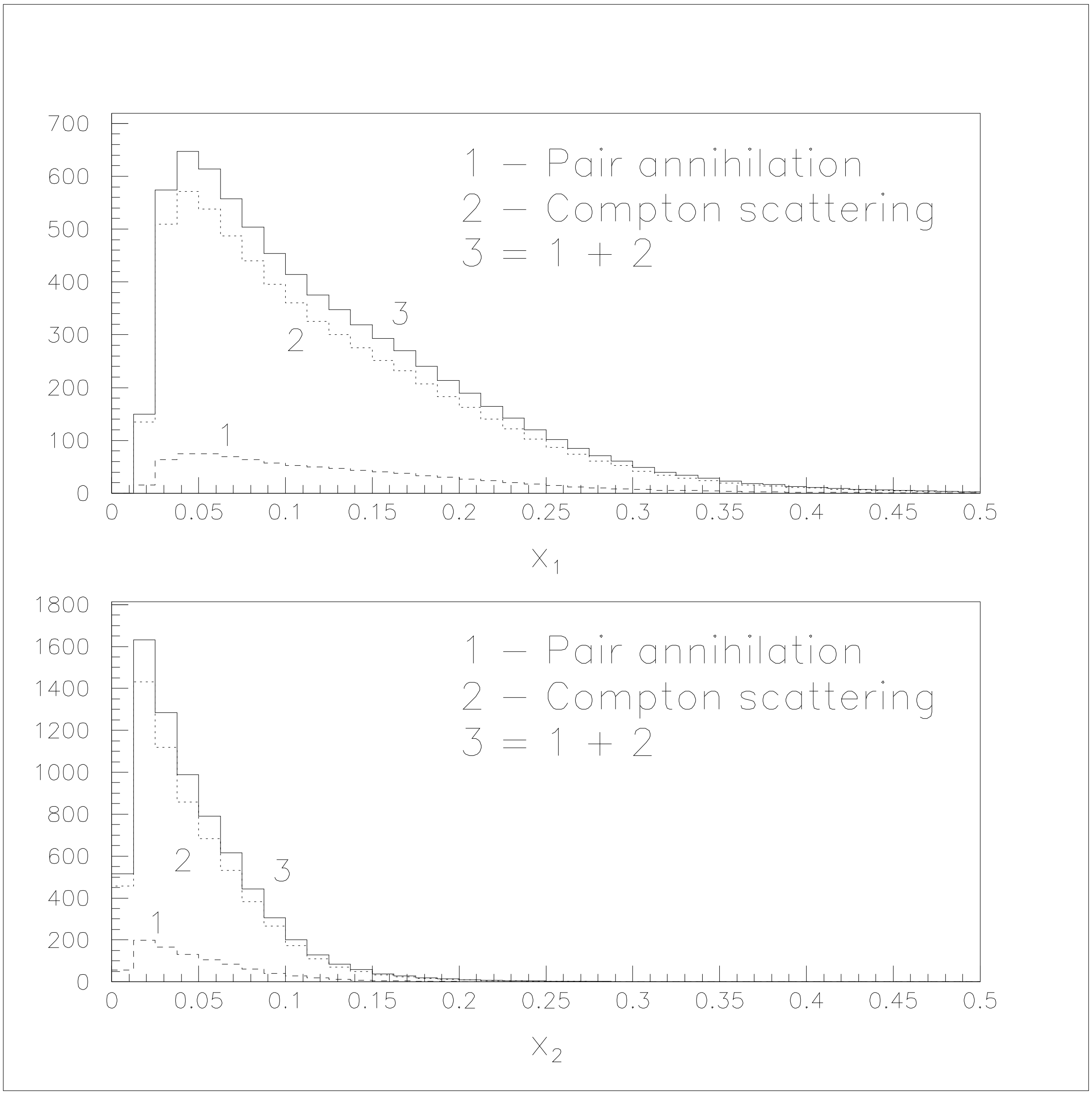

FIG. 3. Momentum fraction x_1 (*top*) and x_2 (*bottom*) distributions from the reaction $pp \rightarrow \gamma + jet$ at pp center of mass energy 500 GeV and $p_t > 10$ GeV in the acceptances of $-1 < \eta_\gamma < 2$ and $-1 < \eta_{jet} < 2$ for photon and jet respectively. The numbers in the vertical axes are cross sections in picobarms. Solid curves – total contribution from pair annihilation and Compton scattering subprocesses, dashed curves – contributions from the $(q\bar{q})$ pair annihilation subprocess, and dotted curves – contributions from the Compton scattering subprocess.

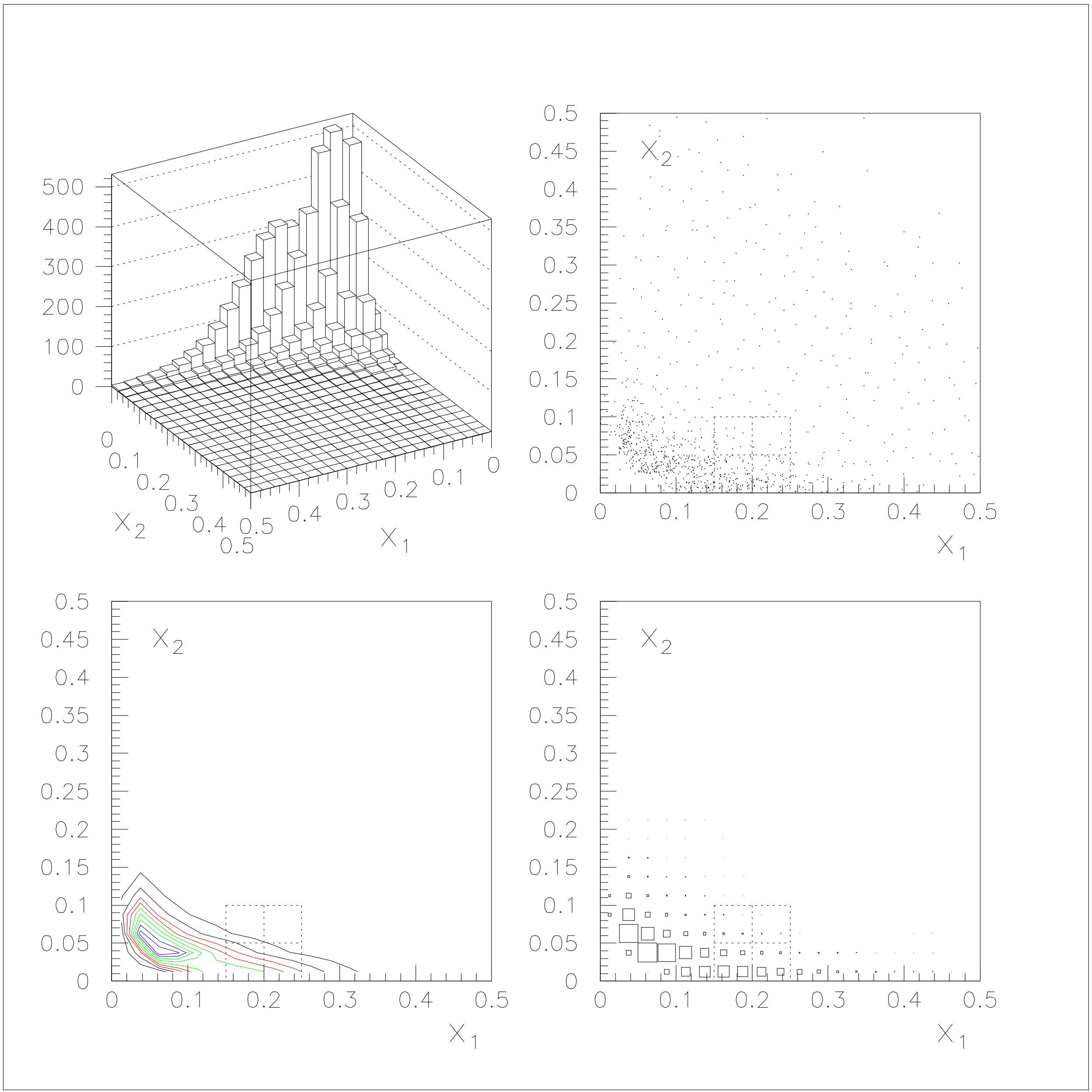

FIG. 4. Two dimentional $(x_1 \times x_2)$ plots for events distribution from the reaction $pp \to \gamma + jet$ at center of mass energy 500 GeV and $p_t > 10$ GeV. The acceptances of the photon and jet are $-1 < \eta_\gamma < 2$ and $-1 < \eta_{jet} < 2$, respectively. The events angular distributions from the four dotted squares with the centers in the points $(x_1, x_2) = (0.175, 0.075)$, $(0.225, 0.075)$, $(0.175, 0.025)$ and $(0.225, 0.025)$ are discussed in this paper.

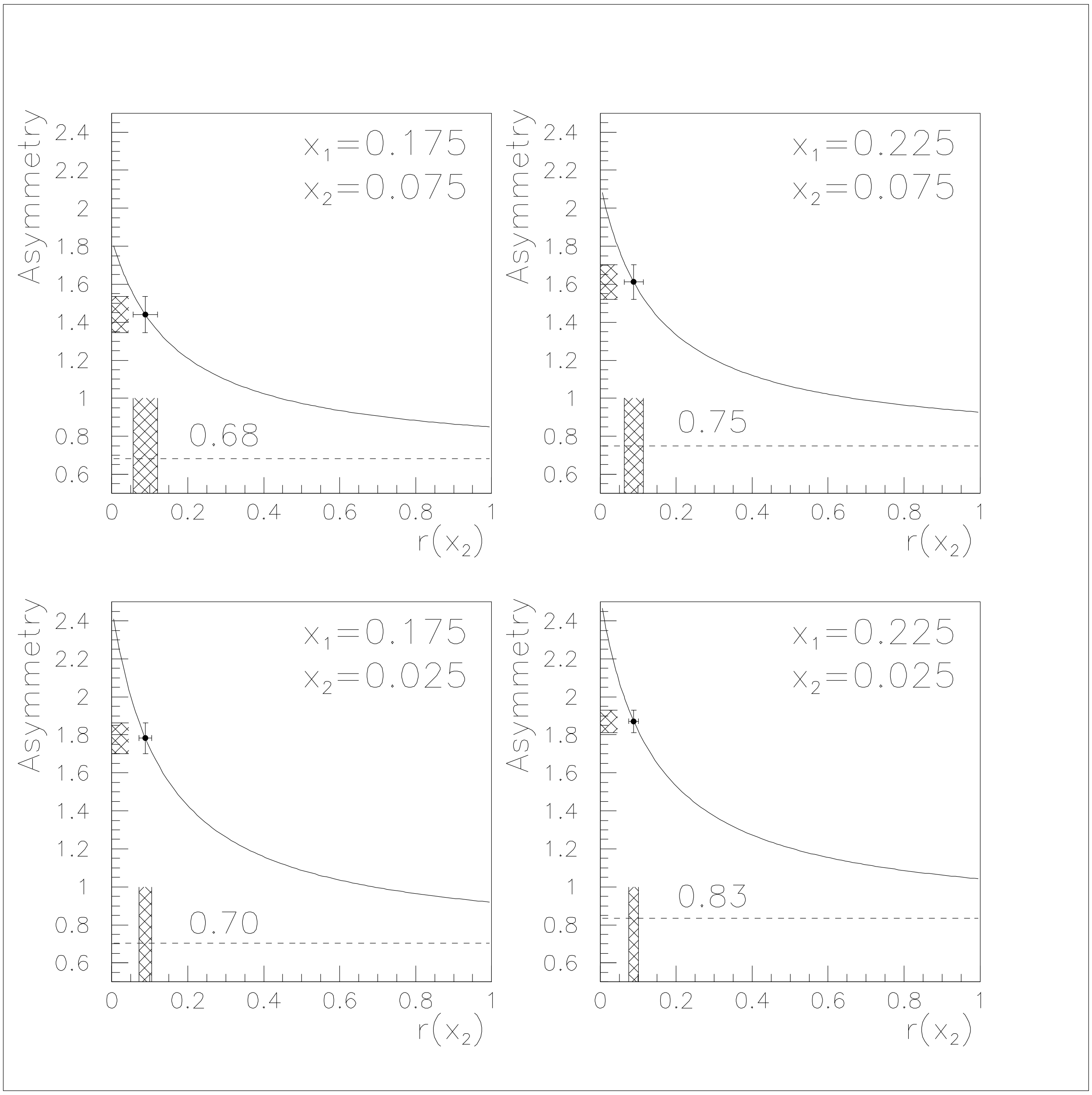

FIG. 5. The $r(x_2)$ dependences of the forward – backward asymmetry $A(x_1, x_2; r(x_2))$ at four points of (x_1, x_2) from the reaction $pp \to \gamma + jet$ at pp center of mass energy 500 GeV and $p_t > 10$ GeV in the acceptances of $-1 < \eta_\gamma < 2$ and $-1 < \eta_{jet} < 2$ for photon and jet respectively: a – $x_1 = 0.175$, $x_2 = 0.075$; b – $x_1 = 0.225$, $x_2 = 0.075$; c – $x_1 = 0.175$, $x_2 = 0.025$ and d – $x_1 = 0.225$, $x_2 = 0.025$. The numbers under the dashed curves are the value of the forward–backward asymmetry at the limit $r(x_2) \gg 1$.

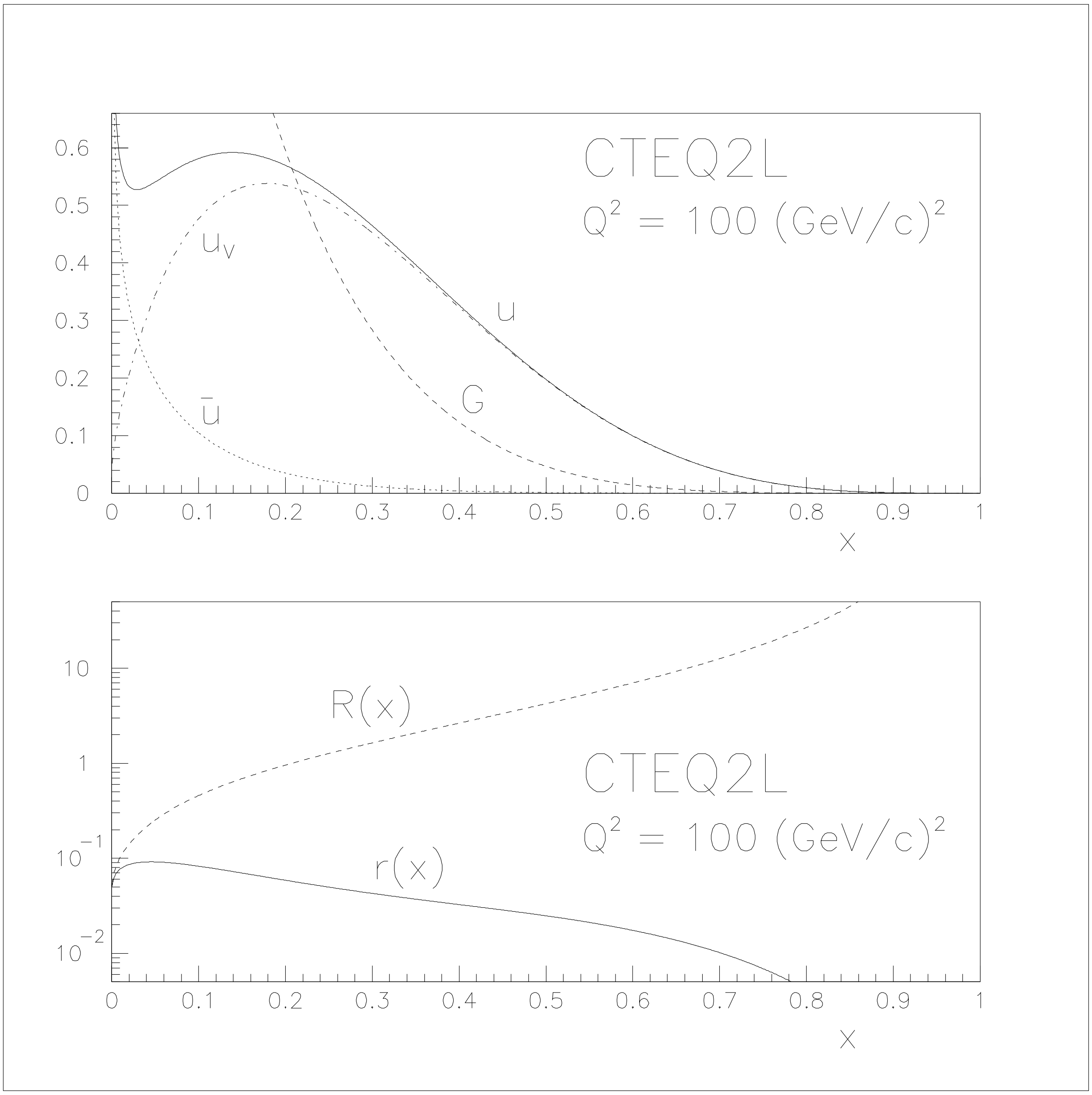

FIG. 6. The distributions of u, $\bar{u}$ quarks and G gluons in the proton multiplied by x (*top*) and functions $r(x)$ and $R(x)$ at $Q^2 = 100\ GeV^2$ from $CTEQ2L$ parametrization (*bottom*). In the *top* figure: solid curve – $xu(x)$ quark distribution, dotted curve – $x\bar{u}(x)$ antiquark distribution, dash–dotted curve – $xu_v(x)$ valence quark distribution and dashed curve – $xG(x)$ gluons distribution; the the *bottom* figure: solid curve – $r(x)$ and dashed curve – $R(x)$.

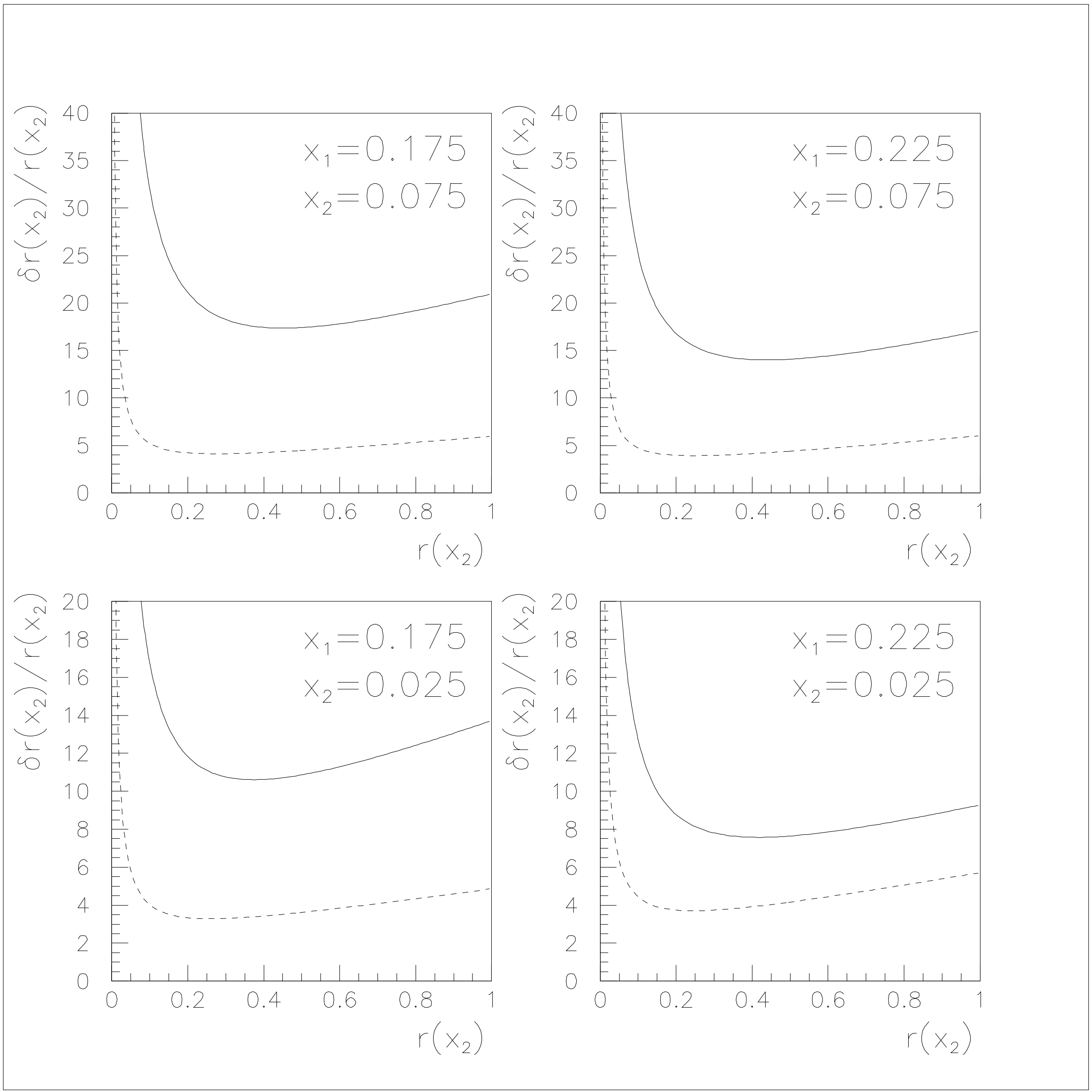

FIG. 7. The $r(x_2)$ dependences of the relative error $\delta r(x_2)/r(x_2)$ in percentages at different points of x_1 and x_2: a – $x_1 = 0.175, x_2 = 0.075$; b – $x_1 = 0.225, x_2 = 0.075$; c – $x_1 = 0.175, x_2 = 0.025$ and d – $x_1 = 0.225, x_2 = 0.025$. At $r(x_2) \simeq 0$ the value of relative error $\delta r(x_2)/r(x_2) \sim r^{-1}(x_2)$, and when $r(x_2) \geq 1$ the value of the relative error $\delta r(x_2)/r(x_2) \sim r(x_2)$. Solid curves – relative error $\delta r(x_2)/r(x_2)$ related with uncertainty of $R(x)$, if $\delta R(x)/R(x) = 10\%$, dashed curves – uncertainty on $r(x_2)$ related with statistical error from asymmetry. The value of the relative error of forward – backward asymmetry $\delta A/A = 1\%$, which would correspond to a standard $STAR$ run.